Journal of Structural Geology 33 (2011) 1334–1346

Contents lists available at ScienceDirect

Journal of Structural Geology

journal homepage: www.elsevier.com/locate/jsg

Ascent and emplacement of pegmatitic melts in a major reverse shear zone (Sierras de Córdoba, Argentina)

Manuel Demartis [a,*], Lucio Pedro Pinotti [a], Jorge Enrique Coniglio [b], Fernando Javier D'Eramo [a], José María Tubía [c], Eugenio Aragón [d], Leonardo Alfredo Agulleiro Insúa [b]

[a] CONICET, Departamento de Geología, Universidad Nacional de Río Cuarto, Ruta Nac. 36 Km. 601, (CP X5804BYA) Río Cuarto, Argentina
[b] Departamento de Geología, Universidad Nacional de Río Cuarto, Ruta Nac. 36 Km. 601, (CP X5804BYA) Río Cuarto, Argentina
[c] Departamento de Geodinámica, Facultad de Ciencia y Tecnología, Universidad del País Vasco, Apartado 644, 48080 Bilbao, Spain
[d] Centro de Investigaciones Geológicas (CONICET - Universidad Nacional de La Plata), Calle 1 N° 644, (CP 1900) La Plata, Argentina

ARTICLE INFO

Article history:
Received 9 March 2011
Received in revised form
8 June 2011
Accepted 26 June 2011
Available online 8 July 2011

Keywords:
LCT pegmatites
Melt ascent and emplacement
Fracture-controlled mechanism
Magma-pumping mechanism
Guacha Corral shear zone

ABSTRACT

Ordovician to Devonian aged crustal-scale Guacha Corral shear zone (GCSZ), central Argentina, hosts rare element pegmatites of the Comechingones pegmatitic field (CPF). In the CPF an eastwards decreasing strain gradient related to the GCSZ deformation is defined, with a high strain domain (HSD) to the west and a low strain domain (LSD) to the east. Pegmatites of the CPF were emplaced in both HSD and LSD synkinematically during ductile GCSZ deformation. Two main mechanisms for pegmatitic melt ascent and emplacement are recognized: "fracture-controlled" and "magma pumping" mechanisms. The former implies fracturing generated due to simple shear deformation not related to any previous heterogeneity. With further deformation, pegmatites were emplaced in low-dip surfaces of anisotropy (C'-planes or T-fractures), that might behave as releasing bends connecting adjacent high-dip conduits or shear zones. Displacements along staggered shear zones with releasing bends induce the local development of domains with negative pressure gradients, where open spaces could form transiently attracting for the collection of buoyant melts, a mechanism similar to "magma pumping". With ongoing deformation pegmatites were progressively rotated, sheared and transposed to the mylonitic foliation. Late pegmatites emplaced by either of the two mechanisms in the HSD and the TZ have retained their original orientations.

1. Introduction

Mineralogical and geochemical studies of granite pegmatites, with emphasis on their petrogenesis and geochemical evolution, have proliferated during recent decades (Černý et al., 1985; London, 1986a,b, 1992; Stern et al., 1986; Černý, 1991a,b; Alfonso et al., 2003; Roda et al., 2004; Galliski and Černý, 2006; Kontak, 2006; Stilling et al., 2006). In contrast, the deformational conditions that control the intrusion and emplacement of pegmatites are only poorly addressed in the literature (Chadwick, 1958; Černý and Brisbin, 1982; Brisbin, 1986; Partington, 1990; Araújo et al., 2001). However, despite the fact that the rheology of pegmatite and granite magmas differs, it seems reasonable that some of the abundant information about the intrusion of granite plutons and dikes could be applied to the intrusion of pegmatite.

Nabelek et al. (2010) stated that high concentrations of volatiles (like Li, B and P) such as those occurring in natural pegmatitic liquids, both reduce viscosity by several orders of magnitude more compared to values used by Baker (1998) and increase the solubility of H_2O in granitic melts, reducing even more the melt viscosity. These effects enhance the mobility of pegmatitic sheets within the crust compared to their parental granites, especially when country rock heterogeneities are available to reduce the magma pressure necessary for propagation of dike fractures.

In this regard, it is now well established that shear zones play an active role in magma transfer throughout the lithosphere, as evidenced by the close spatial relationship between many granite plutons and shear zones (Hutton, 1988; D'Lemos et al., 1992; Neves et al., 1996; Weinberg et al., 2004). It is largely accepted that strike-slip or transpressive tectonic settings provide space for magma emplacement (Druguet and Hutton, 1998; Brown and Solar, 1999; Passarelli et al., 2010).

Less information is available with reference to space generation for granite and pegmatitic melt emplacement in contractional

* Corresponding author. Tel.: +54 358 4676198; fax: +54 358 4680280.
E-mail address: mdemartis@exa.unrc.edu.ar (M. Demartis).

0191-8141/$ – see front matter © 2011 Elsevier Ltd. All rights reserved.
doi:10.1016/j.jsg.2011.06.008

environments. Henderson and Ihlen (2004) demonstrated that the intrusion of pegmatite in the Bamble terrane (southern Norway) was linked to a major event of contractional deformation. According to these authors, the Bamble terrane provides a good example of pegmatite intrusion related to an orthogonal orogenic deformation, the pegmatites being emplaced in axial planar joints related to folding of the metamorphic country rocks.

Many authors suggested that the content of volatile dissolved in granitic magmas strongly influences their viscosity. Dingwell et al. (1996) reported that the granitic melt viscosity decreases more than two orders of magnitude at 800 °C as the content of P, B, K, Na, Li or F increased from 0 to 5% weight in the melt. The concentration of such elements up to near 1 wt% in granitic melts, which usually takes place during the granite–pegmatite transition, results in local overpressures promoting the development of hydraulic fractures at the intrusion tip. Such an interplay between compositional and fracturing processes works like a feedback mechanism that helps the ascent of the pegmatitic melt.

This paper deals with the structural evolution of synkinematic pegmatites emplaced in a contractional deformation field. The studied region is located in the southeastern corner of the Sierras Pampeanas, in central Argentina, where a large amount of Be–P–Nb–Ta–U-bearing pegmatites, grouped by Galliski (1994) in the so-called Comechingones Pegmatitic Field (CPF), crops out (Fig. 1a and b). These pegmatites were emplaced at pressures of approximately 500 MPa, associated with the crustal scale Guacha Corral shear zone (GCSZ; Demartis, 2010). Our interpretations are based on detailed mapping and structural studies of two pegmatite-rich sectors, corresponding to weakly and strongly deformed domains of the GCSZ (Fig. 1c). The aim of such a selection is to obtain reliable information on the emplacement mechanism of the pegmatites, as well as on their subsequent evolution. At first sight, the transfer of magma through such a ductile, middle-pressure continental crust seems to require a huge amount of energy. However, we will show that: 1) deformation along the GCSZ provided open spaces for the migration and ascent of pegmatite melts, and 2) the high volatile content of the Comechingones pegmatites significantly enhanced the buoyant force of these pegmatitic melts. These two points suggest a mechanism of easy intrusion for the pegmatites through the ductile continental crust. This alternative model for mass transfer within the ductile crust contributes to solve the energetic and rheological problems of volatile-rich-melt ascent from lower to middle crustal zones.

2. The Comechingones pegmatitic field (CPF)

Pegmatites of the CPF correspond to the Li-, Cs- and Ta-bearing pegmatites (LCT) of Černý and Ercit (2005), and are classified as muscovite- and rare element-class, beryl-columbite-phosphate-subtype pegmatites (Galliski, 1994). Regional mapping of the pegmatite field was performed through ASTER images. Quartz- or silica-rich rocks display a characteristic spectral signature in the thermal spectral region (Rowan and Mars, 2003; Ninomiya, 2004), and ASTER thermal infrared (TIR) bands were successfully used to recognize large outcrops of granite pegmatites.

The following textural and mineralogical zonations are frequently observed in each pegmatitic sheet: fine- to medium-grained muscovite + quartz + albite in the border zone; medium- to coarse-grained quartz + muscovite ± microcline ± albite in the wall zone; coarse- to very coarse-grained graphic microcline + quartz + muscovite ± albite in the intermediate zone (in some cases an additional intermediate zone exists, almost completely composed of blocky perthitic K-feldspar); finally, a core zone, with quartz, and minor and variable amounts of very coarse-grained microcline and muscovite. Garnet, triplite-zwieselite, uraninite and its secondary products, beryl, and columbite-tantalite minerals are the most common accessory minerals, generally occurring in the intermediate and core zones. Several geochemical ratios, such as low K/Rb and K/Cs values in alkali feldspars from core zones (Demartis, 2010), point to intermediate to highly evolved pegmatites. Extremely highly fractionated replacement units with albite, Li-mica, amblygonite and accessory minerals such as Hf-rich zircons, Ta and Mn-rich columbites, and microlites, also occur in some pegmatites (Demartis et al., 2011). Pegmatite crystallization occurs at pressures of *ca.* 500 MPa and temperatures of 600–700 °C, according to fluid inclusion and stable isotope studies (Demartis, 2010).

3. Geological setting

The Sierras de Córdoba, in central Argentina, form the southern branch of the Sierras Pampeanas (Fig. 1a). They encompass several N-trending blocks of pre-Andean basement that were uplifted by Tertiary reverse faults. These mountains mainly include metasedimentary and igneous rocks of Precambrian to Carboniferous age, locally covered by discordant sedimentary and volcanosedimentary sequences of Late Carboniferous, Permian, Cretaceous, and Tertiary ages. Two major pre-Carboniferous orogenies took place in the Sierras Pampeanas (Rapela et al., 1998, 2001; Otamendi et al., 2004). The oldest one, referred to as the Pampean orogeny, developed between Neoproterozoic and Cambrian times; it was associated with a medium-grade metamorphism, the M1-D1 event, leading to the formation of ortho- and para-gneiss, marble, and amphibolite (Rapela et al., 1998; Otamendi et al., 2004). A subsequent tectono-metamorphic event, M2-D2, is characterized by upper amphibolite to granulite metamorphic rocks, formed under temperatures of ~750 °C and pressures of 650–700 MPa. During this event, granites and migmatites with stromatitic and nebulitic structures (Otamendi et al., 2004; Fagiano, 2007) were produced by partial melting of metasedimentary protoliths. The dominant foliation, S2, and compositional banding in gneisses and migmatites are usually parallel to the oldest residual foliation, S1, and they strike commonly between N300° and 350° E, and dip moderately toward the E (Fagiano, 2007).

The Famatinian orogeny, spreading from Ordovician to Devonian times, greatly reworked the Pampean fabrics, especially along several major shear zones of the Sierras de Córdoba. The GCSZ (Fig. 1b) is the largest and most complex shear zone of the Sierras de Córdoba (Martino, 2003; Whitmeyer and Simpson, 2003; Fagiano, 2007). Large, late to post-Famatinian granite batholiths, like the Cerro Áspero (CAB) and Achala (AB) batholiths (Fig. 1b), intrude in the GCSZ. They produce thermal aureoles on mylonites, evidencing their post-tectonic intrusion (Pinotti et al., 2006).

The GCSZ is a ~120 km long by 20 km wide shear belt that crops out in the Sierra de Comechingones, with a N–S trend and moderate (~30°) eastward dip (Fig. 1b). GCSZ deformation evolved from ductile to (ductile)-brittle conditions. Initial medium- to high-amphibolite facies conditions, represented by biotite- and sillimanite-bearing mylonitic rocks ($M3_a$-$D3_a$ event), were replaced by greenschist facies assemblages ($M3_b$-$D3_b$) leading locally to the formation of chlorite- and sericite-bearing phyllonites (Fagiano, 2007).

Mylonitic rocks in the GCSZ are characterized by a fine-grained matrix composed of recrystallizated biotite + quartz + feldspar + sillimanite. The parallel arrangement of these minerals defines the S3 mylonitic foliation that wraps around garnet porphyroclasts (0.2–2.0 mm in diameter) and quartz + feldspar aggregates. Most authors agree that the GCSZ produced a top-to-the-west sense of shear (Whitmeyer and Simpson, 2003; Fagiano, 2007). In many places, the $M3_b$-$D3_b$ retrograde event is evidenced by the transformation of biotite into chlorite and/or muscovite, and by the

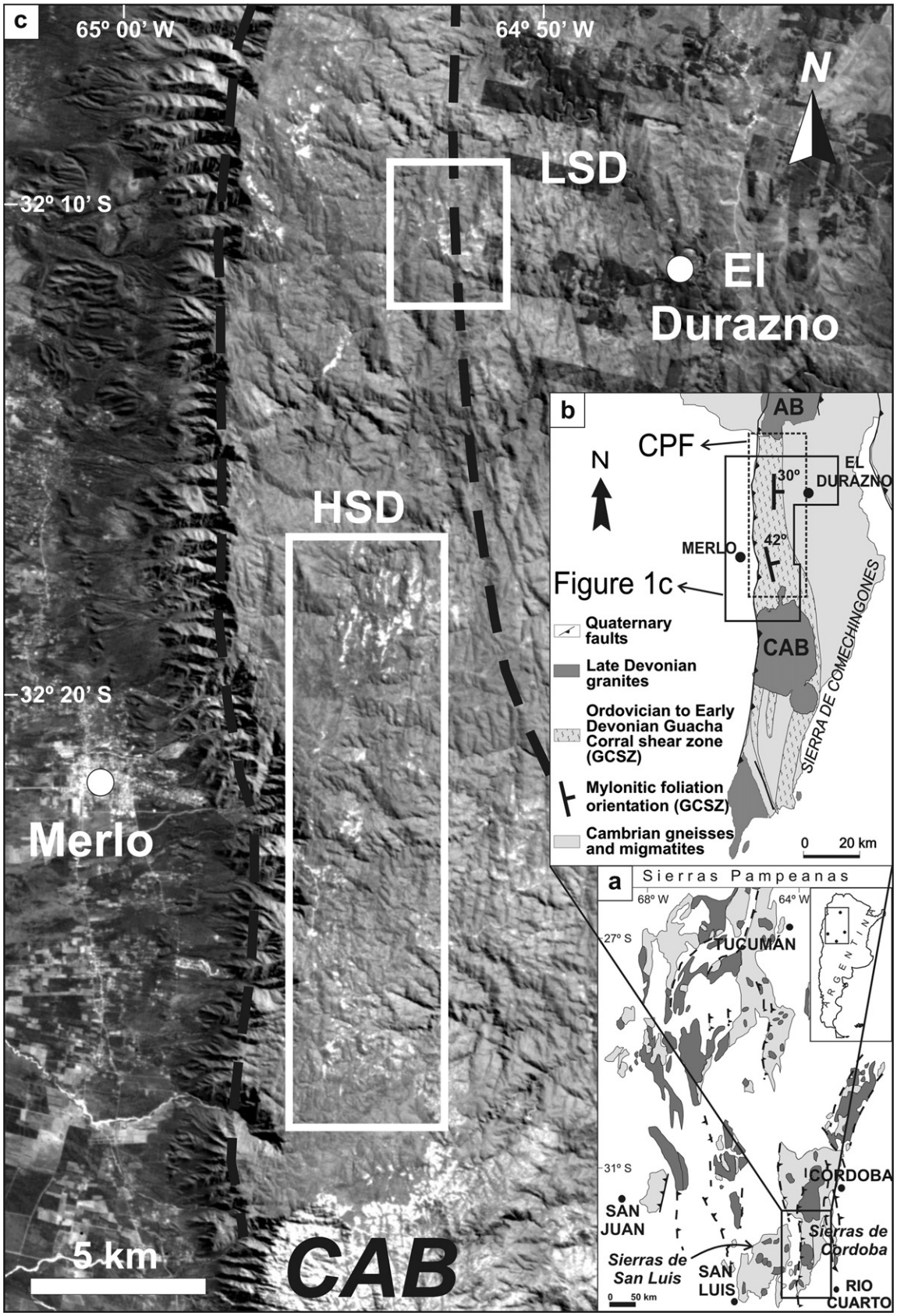

Fig. 1. a) Geological sketch of the Sierras Pampeanas, Argentina, showing the position of the Sierra de Comechingones. b) Simplified geological map of the Sierra de Comechingones showing the extent of the Guacha Corral Shear Zone (GCSZ). The heavily lined polygon corresponds to the extension of the studied area amplified in Fig. 1c, and the dashed rectangle corresponds to the Comechingones Pegmatitic Field (CPF). CAB: Cerro Áspero Batholith; AB: Achala Batholith. c) CBERS satellite image of the studied area, where the High Strain Domain (HSD) and the Low Strain Domain (LSD) are represented in Figs. 2 and 3, respectively. The boundaries of the GCSZ are marked by broken lines.

development of centimeter-scale chevron folds on the mylonitic foliation.

Whitmeyer and Simpson (2003) interpret the GCSZ as the southern part of a larger fault zone termed the "Tres Árboles Fault Zone." These authors also consider that the GCSZ placed into contact Cambrian rocks from the eastern hanging-wall block over Ordovician materials of the westward footwall block, along more than 250 km at the western margin of the Sierras de Córdoba. The regional extension of the GCSZ and kinematics reveal that it constitutes a contractional shear zone at the crustal scale. This study is based on structural data from two domains (Figs. 1, 2 and 3), chosen for their high content in pegmatitic bodies and making up a complete E–W transect across the GCSZ.

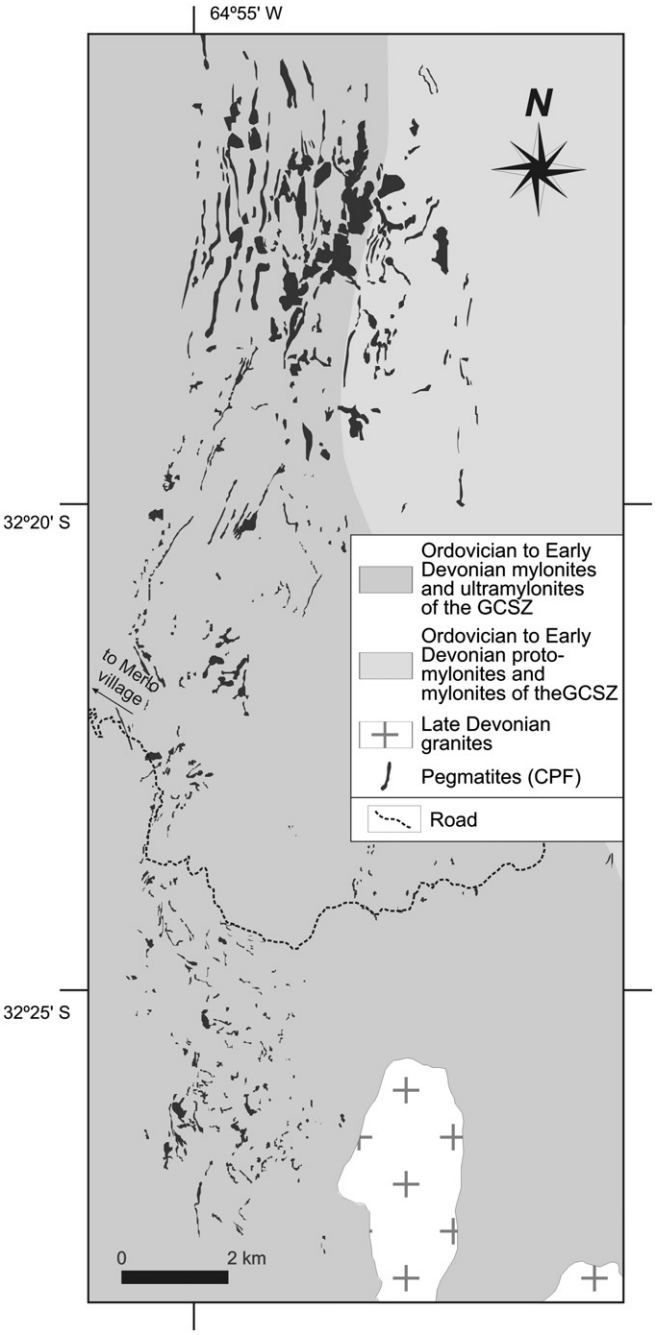

Fig. 2. Lithological map of the HSD. GCSZ: Guacha Corral Shear Zone.

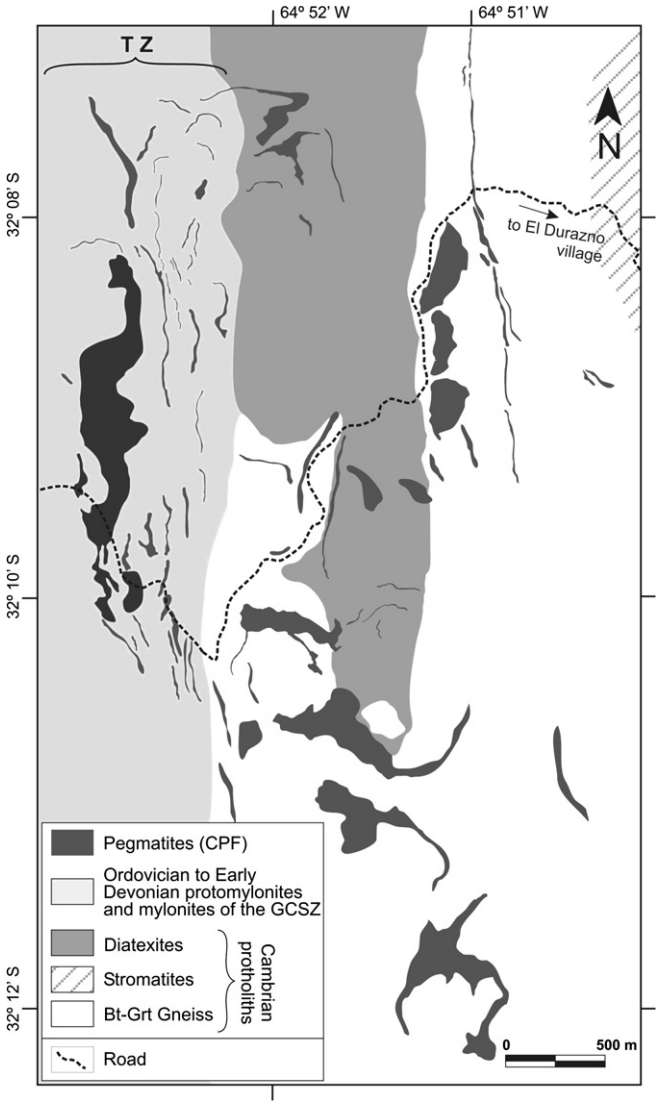

Fig. 3. Lithological map of the LSD. TZ: Transition Zone.

4. Structural analysis

Pegmatites are found as countless lens- or sheet-shaped bodies of relatively small size (less than 50 m thick and 200 m long). Pegmatitic sheets frequently come into contact, forming larger bodies (Fig. 4) thicker than 200 m and longer than 1 km. In many outcrops, several magmatic pulses coalesce to form an apparently single intrusion. However, even in these cases it is possible to recognize the composite nature of such bodies, as each pegmatitic sheet tends to preserve its internal zonation (Fig. 5a).

The mylonitic foliation of the country rocks wraps around the pegmatite bodies (Fig. 5a) very often, suggesting that the behavior of the pegmatite was harder than that of the country rocks during deformational events active after the crystallization of the pegmatite melt. In contrast, other pegmatitic bodies deflect the foliation of the country rocks (Fig. 5b), which point to local distortions of the mylonitic foliation promoted by the overpressure of the pegmatitic melts. Slices of mylonitic rocks are frequently sandwiched between undeformed (and deformed, less often) pegmatitic bodies (Fig. 5c).

Geological and structural data reveal a pronounced strain gradient, marked by a progressive grain-size reduction of mylonitic

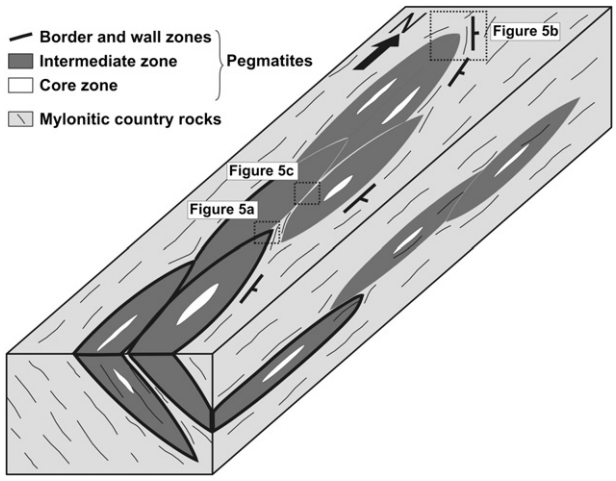

Fig. 4. 3D schematic block-diagram showing multiple, lens-shaped pegmatitic sheets emplaced beside each other forming larger tabular pegmatitic bodies, deflecting the mylonitic foliation of the country rock. Dashed rectangles represent the photographic field locations shown in Fig. 5. See main text for further explanation.

rocks toward the basal contact of the GCSZ. In the western domain, close to Merlo village (Figs. 1c and 2), the gneissic and migmatitic fabrics associated with the Pampean orogeny are almost completely obliterated by the mylonitization; this sector is described as the "High Strain Domain" (HSD). In contrast, the Pampean protholiths predominate over the Famatinian mylonites in the northeastern part of the studied area, near El Durazno village (Figs. 1c and 3), here referred to as the "Low Strain Domain" (LSD). Biotite- and garnet-bearing banded gneisses are the most common lithologies in the LSD. Migmatites with nebulitic and stromatic structures are also present in the LSD and usually grade transitionally into Bt-Grt gneisses. In this domain, the effect of the Famatinian deformation is weak, as only few centimeter- to meter-sized protomylonitic shear bands are observed isolated within large blocks of older gneisses and migmatites. The western margin of the LSD is a 1 km-wide shear zone, which we interpret as a transitional zone (TZ) between the HSD and the LSD. Mylonitic rocks in the TZ are coarser grained and scarcer than in the HSD. Structural analysis in the two domains involves conventional measurements of all field structures observed in both country rocks and pegmatites. In order to determine the mean planar orientation of each pegmatite, several measurements along pegmatite-country rock contacts were taken and then averaged. This work also included microstructural and kinematic data from XZ-thin sections.

4.1. High strain domain

About 85% of the pegmatite outcrops from the CPF are found in the HSD. In this domain, the mylonitic foliation shows a mean N354° E strike and dips 46° E (Fig. 6a). However, throughout the HSD the orientation of mylonitic foliation varies, outlining almond patterns at the regional scale (Fig. 6a). Poles to the mylonitic foliation from this northern sector outline a single girdle whose π-axis plunges approximately 18° N (Fig. 6a; uppermost stereoplot). The analysis of this stereographic plot is consistent with the presence of upright, asymmetric chevron folds that deform the mylonitic foliation in the HSD. These centimetric- to kilometric-sized folds are devoid of axial planar foliation. Because of these reasons, we link these folds to a late folding event related to the retrograde event $M3_b$-$D3_b$.

A stretching lineation is defined by the parallel arrangement of sillimanite needles, feldspar porphyroclasts, quartz aggregates, and micas. This lineation plunges moderately (40°) to the ENE (Fig. 6a). Kinematic criteria attest to an almost reverse sense of shearing, consistent with tectonic transport toward the WSW for the hanging-wall block postulated previously in other sectors of the GCSZ (Simpson et al., 2003; Whitmeyer and Simpson, 2003; Fagiano, 2007).

Pegmatitic bodies display a lenticular shape, frequently with the length six times greater than the thickness. Mean pegmatite planar orientation from the two domains is summarized in Table 1, mostly striking 345° E and dipping moderately to the E, concordant with mylonitic foliation (Fig. 6b). Minor discordant pegmatites also exist, mainly at the northern part of the HSD. These are at a high angle to the mylonitic foliation, having 022° E strikes and 55° W dips (Figs. 5d and 6b). The pegmatites from the HSD frequently display a foliation defined by flattened porphyroclasts of coarse-grained microcline, quartz, and muscovite. This foliation is usually parallel to the mylonitic foliation of the country rocks (Figs. 5e and 6b) and to the axial surface of tight folds observed in some pegmatite sheets (Fig. 5f).

The mylonitic country rocks from the HSD contain garnet, plagioclase, K-feldspar, and quartz porphyroclasts. These porphyroclasts usually show sigma and delta morphologies with reorientation, recrystallization, and migration of matrix minerals toward pressure shadows. S and C planes in S/C microstructures are nearly parallel. Fine-grained feldspars are also observed associated with <100 μm-diameter biotite + quartz matrix recrystallized minerals. Both biotite and sillimanite of the matrix are recrystallized and transposed parallel to the mylonitic foliation during shearing. Newly formed biotite is considerably smaller than the relict one of the gneissic and migmatitic protholiths. Prismatic sillimanite is almost completely transformed into fibrolite. Quartz usually forms ribbons parallel to the mylonitic foliation, and experiments grain boundary migration and bulging dynamic recrystallization.

Textures and microstructures in all internal zones of pegmatites from the HSD show evidence of deformation in a large range of temperatures, from submagmatic to subsolidus at low-temperature. Many large feldspar porphyroclasts present wedge-shaped intracrystalline fractures filled with medium- to fine-grained aggregates of quartz + muscovite ± microcline (Fig. 7a and b). These mineral aggregates are interpreted as coming from the residual melt that intruded the intracrystalline fractures that developed during submagmatic-state deformations (Bouchez et al., 1992). Mechanical twins in feldspar and chessboard microstructures in quartz account for high-temperature subsolidus deformation. As quoted by Stipp et al. (2002), dynamic recrystallization by grain boundary migration in quartz, as may be observed from Fig. 7c, develops above 500–550 °C, generating lobate grain boundaries and interfingered grain contacts. Albitic perthites with flame shapes in large microcline grains (Fig. 7d) also occur during subsolidus-state deformation at medium-temperature conditions, and this has been observed mostly in intermediate zones of pegmatites. Finally, deformation lamellae and undulose extinction in quartz grains from all internal zones of the pegmatites indicate that late deformations under low-temperature conditions also occurred in the pegmatites. These textures and microstructures point to a continuum of deformation of the pegmatites, starting under submagmatic conditions and ending with low-temperature deformations.

4.2. Low strain domain (LSD)

Country rocks in the LSD are mostly Pampean gneisses and migmatites, with a weak imprint of younger Famatinian deformation. The Pampean S2 foliation is deformed by centimeter- to

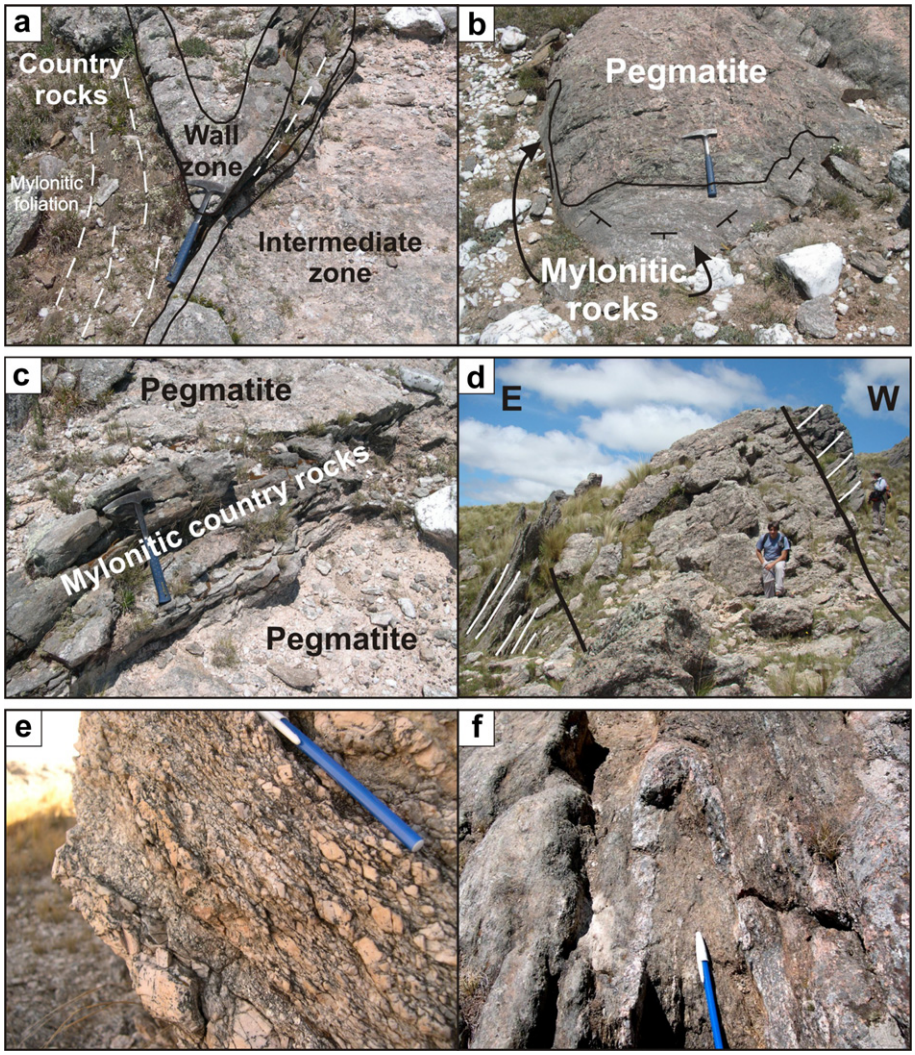

Fig. 5. Photographs showing field relationships among different lens-shaped pegmatitic bodies (see localization of photographs in Fig. 4). The hammer is 35 cm long. a) Internal petrographic zoning preserved in two stacked pegmatitic lenses. The mylonitic foliation of the country rocks accommodates to the tip of the upper pegmatite lens. b) Tip of a lenticular pegmatitic body, where mylonitic foliation was deformed during the forced intrusion of the melt. c) Slice of country rocks between two pegmatitic bodies. d) Westward-dipping pegmatite intruding discordantly the mylonitic country rocks. e) Intermediate zone of a pegmatite showing mylonitic foliation. Stretched and reoriented microclines, quartz ribbons, and oriented micas can clearly be recognized. The pen is 15 cm long. f) Pegmatite from the HSD showing a tight fold whose axial surface is parallel to the foliation of the country rocks.

meter- and kilometer-scale folds developed during the D2 tectonothermal event of the Pampean orogeny. These folds, with tight to isoclinal profiles, and moderate plunge to the SSE of their fold axes (Fig. 8a), are best expressed in gneisses and migmatites from parts of the Sierras de Córdoba with no imprint of deformation related to the GCSZ (Otamendi et al., 2004; Fagiano, 2007). However, they are also preserved in protomylonites of the TZ, where the Famatinian deformation did not completely obliterate the older Pampean structures.

All over the LSD, the foliation of gneiss, migmatite and mylonite shares a common orientation: N340°–N350° E in strike and ~60° E in dip (Fig. 8a). An eastward-plunging mineral-stretching lineation was also measured in the mylonitic (and protomylonitic) rocks of the TZ, where a reverse sense of shear is denoted by sigma-porphyroclasts.

Contrary to the HSD, the mylonites, gneisses and migmatites in the LSD display microstructures with only slightly stretched garnet, quartz and plagioclase porphyroclasts occasionally showing sigma- and delta-morphologies. Partially recrystallised quartz, biotite and sillimanite grains occupy the porphyroclast pressure shadows. Sillimanite grains still remain prismatic but moderately fragmented. Quartz grains display chessboard microstructures and experienced recrystallization by grain boundary migration. S/C microstructures cannot be distinguished as clearly as in the mylonitic rocks.

In the easternmost part of the LSD the pegmatite bodies are mostly discordant, generally with N–S strikes and eastwards dips, but with two different mean dips: sheets with <40° E dips are dominant but a minor group with >70° E dips is also recognized (Table 1; Fig. 8b, upper stereoplot). The low-dip ones are thicker (generally between 20 and 50 m thick) than the steep-dip ones (Fig. 9). The geometry of the pegmatites from the LSD is essentially tabular. Most of them appear as roughly E-elongate outcrops on the geological map (Fig. 3); however, such an elongation is apparent, since it only reflects the intersection of flat-dipping bodies with the E–W oriented valleys that are common in this region. The pegmatite bodies from the TZ are concordant with the mylonitic foliation. Both planar orientation of pegmatites and mylonitic foliation show approximately N–S strikes and moderate dips to the east (Fig. 8b and Table 1). Some pegmatitic bodies cross-cut the

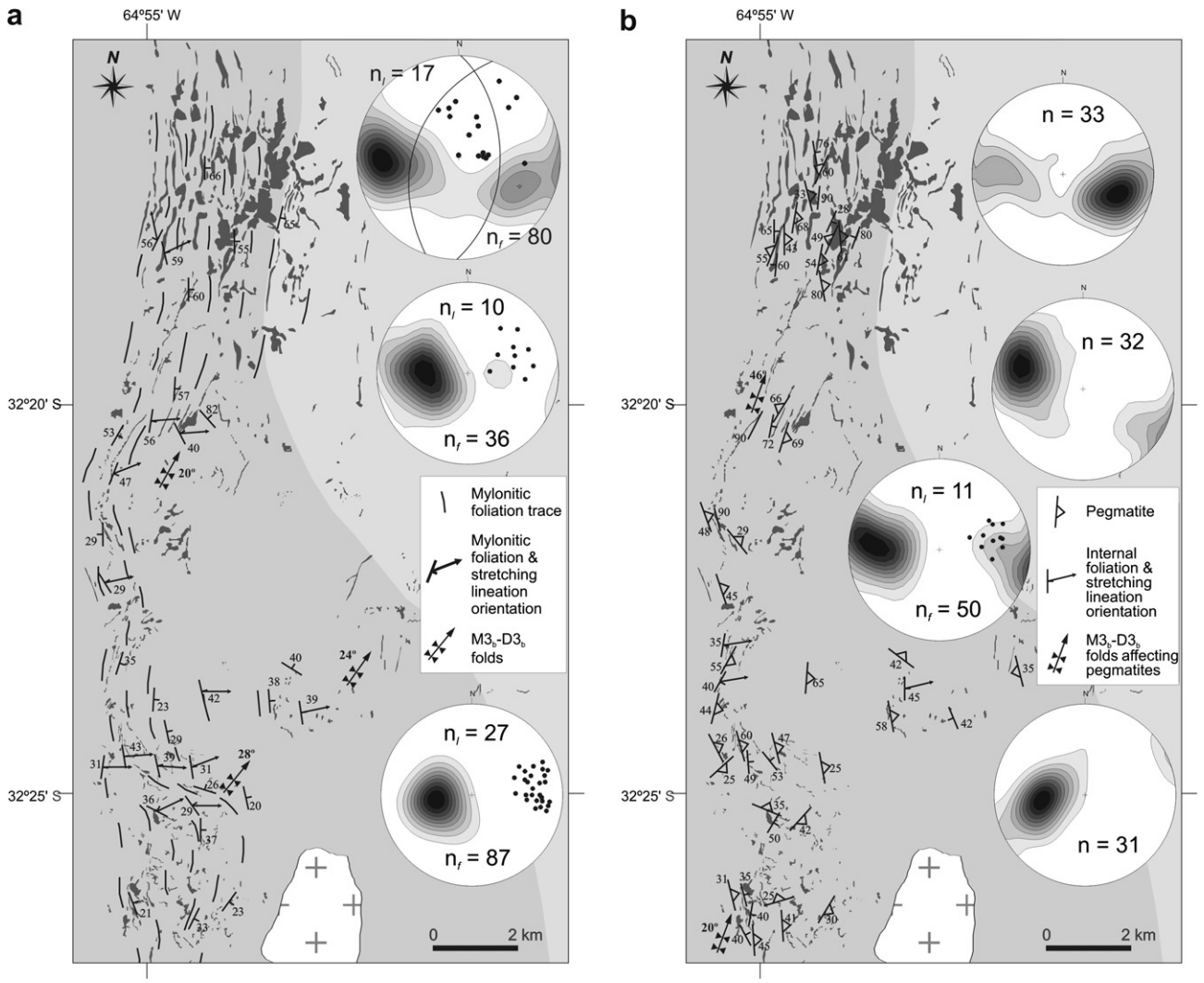

Fig. 6. Structural maps of the HSD. a) Mylonitic foliation traces and lower-hemisphere stereograms showing poles to mylonitic foliation planes (density diagrams) and mineral-stretching lineation (dots) in northern, central, and southern parts of the HSD. The mylonitic foliation is curved because of the kilometer-scale folding that took place during the $M3_b$-$D3_b$ retrograde event. b) Orientation of pegmatite-country rock contacts and lower-hemisphere stereograms (density diagrams) of the northern, central, and southern parts of the HSD. Internal foliation (density diagram) and mineral-stretching lineation (dots) development in pegmatitc rocks are also shown in the lower-hemisphere stereograms. n_f and n_l: number of foliation and lineation measurements, respectively. Lithological references as in Fig. 2.

mylonitic foliation and the Pampean regional folds. These bodies also strike N–S but their dip is moderate to the west (Fig. 8b and Table 1). Rare pegmatites have ~E–W strikes and steep dips.

An internal tectonic foliation and a mineral-stretching lineation also develop in the LSD pegmatites (Fig. 8b), and the kinematic markers indicate a reverse sense of shear like in the mylonitic country rocks. Since the pegmatites from the LSD and the TZ also display submagmatic to low-temperature subsolidus textures and microstructures we argue that all the pegmatites were emplaced synkinematically.

Table 1
Mean orientations of pegmatitic bodies in the "High Strain Domain" (HSD), "Transition Zone" (TZ), and "Low Strain Domain" (LSD), used for the structural analysis and emplacement modeling.

HSD	TZ	LSD
- Concordant pegmatites N-345° striking/44° E dipping	- Concordant pegmatites N-011° striking/57° E dipping	- Low-dipping angle pegmatites N-005° striking/22° E dipping
- Discordant pegmatites N-022° striking/55° W dipping	- Discordant pegmatites N-002° striking/37° W dipping	- High-dipping angle pegmatites N-355° striking/ 79° E dipping

5. Discussion

5.1. Synkinematic emplacement of pegmatites

Development of a mylonitic foliation, stretching lineations, and folds in the pegmatite sheets, with similar orientations and the same kinematics as those observed in the metamorphic country rocks demonstrate that they were deformed during the ductile $M3_a$-$D3_a$ event in the deformational evolution of the GCSZ. The preservation of microstructures recording a complete evolution from submagmatic to low-temperature deformations further attests to the synkinematic emplacement of the CPF during the $M3_a$-$D3_a$ event.

The orientation of the shear zone and the sense of shear are consistent with a reverse, top-to-west motion of the GCSZ (Figs. 2

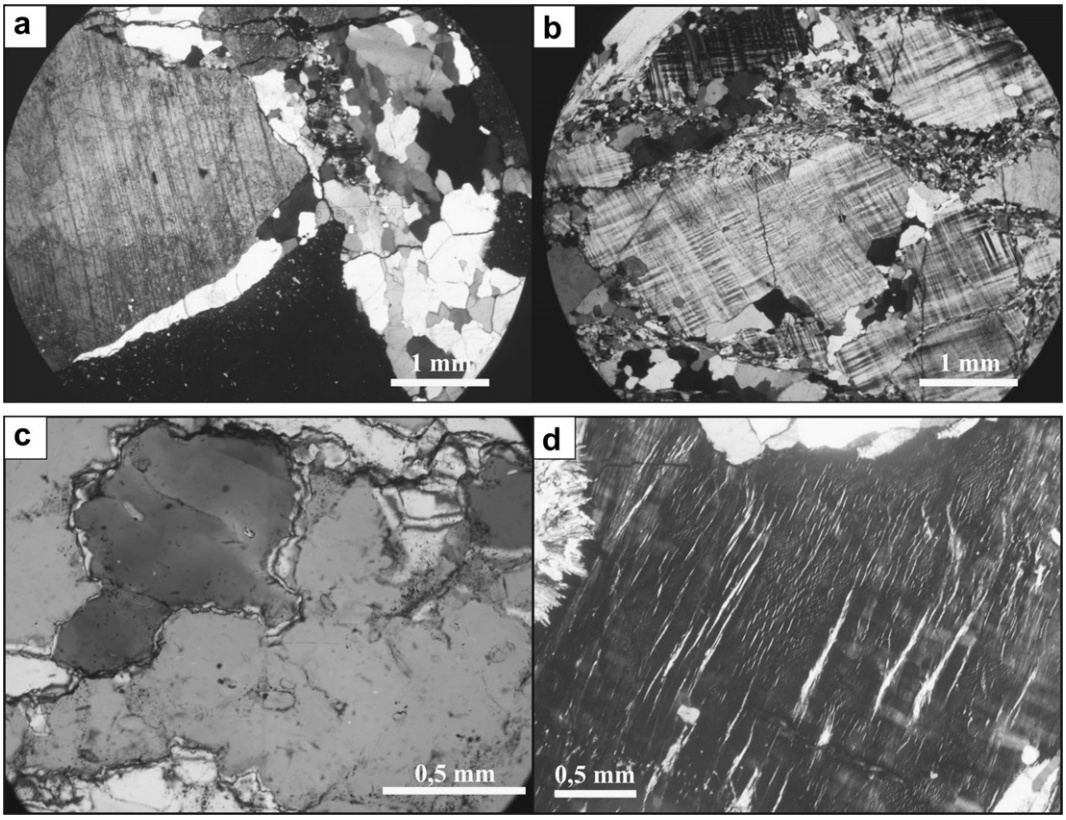

Fig. 7. a) Wedge-shaped intracrystalline fracture in feldspars from the intermediate zone of a pegmatitic body, infilled with a residual melt composed of strongly recrystallized quartz and minor fine-grained feldspars and muscovite. Note that quartz grains are optically continuous from the inside to the outside of the fracture. The large feldspar grain is fractured and subdivided into two sub-grains, one of which was rotated from its original position. Crossed polarizers, XZ-section. b) Network of intracrystalline fractures affecting a large microcline grain, also infilled by variably recrystallized quartz, muscovite, and feldspar. The resulting microcline fragments are also rotated. Crossed polarizers. c) Lobated quartz grain boundaries and interfingered grain contacts denoting dynamic recrystallization and grain boundary migration. Crossed polarizers. d) Albite flame perthites in large microcline grain from the intermediate zone of a pegmatitic body. Crossed polarizers.

and 4), as previously established by Simpson et al. (2003), Whitmeyer and Simpson (2003), Martino (2003) and Fagiano (2007). The systematic asymmetry of the kinematic markers all along the shear zone points to a deformation mechanism close to simple shear. These observations allow us to propose that a compressive stress field, where σ_1 and σ_2 axes are subhorizontal, and E- and N-trending, respectively (Fig. 10), are responsible for pegmatite emplacement. Space generation in a contractional setting is non-intuitive. We contend that the development of a crustal-scale reverse shear zone was the most important factor controlling the generation of spaces. Two main mechanisms for magma ascent and emplacement are proposed: (1) fracture-controlled related to simple shear, and (2) magma pumping within a mylonitic carpet.

5.2. Fracture-controlled emplacement

Interrelations between shearing and magma emplacement have been the subject of considerable documentation. Fracture-controlled ascent of magma in a ductile crust has been explained by melt-enhanced embrittlement (Davidson et al., 1994; Brown and Solar, 1998a) and ductile fracturing (Weinberg and Regenauer-Lieb, 2010). According to these mechanisms, deformation and partial melting interact through positive feedback cycles. Fracturation of the country rocks takes place when percolative flow is not effective in expelling the interstitial partial melts, the accumulated magma reaching a high enough pressure to overcome the ductile behavior of the crust.

Many authors have established that shearing was the main process controlling both magma ascent and emplacement or melting and expulsion of magmas from their source regions (D'Lemos et al., 1992; Vigneresse, 1995; Brown and Solar, 1998b; Druguet and Hutton, 1998; Leitch and Weinberg, 2002; Rosenberg, 2004; Denèle et al., 2008; Burda and Gawęda, 2009; Passarelli et al., 2010). However, Neves and Vauchez (1995) suggested an alternative explanation for the spatial association of granites and strike-slip shear zones in the Borborema Province, Brazil. They propose that shear zones nucleate due to thermal anomalies associated with preexisting magma chambers, thus confirming a magmatically influenced shear zone development. Subsequently, Neves et al. (1996) presented field, anisotropy of magnetic susceptibility, petrographic, and geochemical data from many granitoids from the Borborema Province, supporting the theory of both shear zone-controlled magma emplacement and magma-assisted nucleation of shear zones. Corti et al. (2002) also concluded that strain distribution and structural evolution can be controlled by the presence of magma at depth in extensional settings. They state that thermal weakening of country rocks leads to positive feedback interactions between magma and deformation. The arguments presented here allow us to conclude that both scenarios are possible.

The GCSZ provides multiple conduits for magma ascent and transport throughout the middle continental crust. Many pegmatites that outcrop discordantly in the HSD, TZ, and LSD are here regarded as magmas emplaced in fractures that were developed in response to simple shear deformation (Fig. 10), with no particular relationship with a pre-existing anisotropy. The thick and low-dip pegmatites that appear on the LSD are viewed as representing magmas intruded in fractures at right angle to the minimum

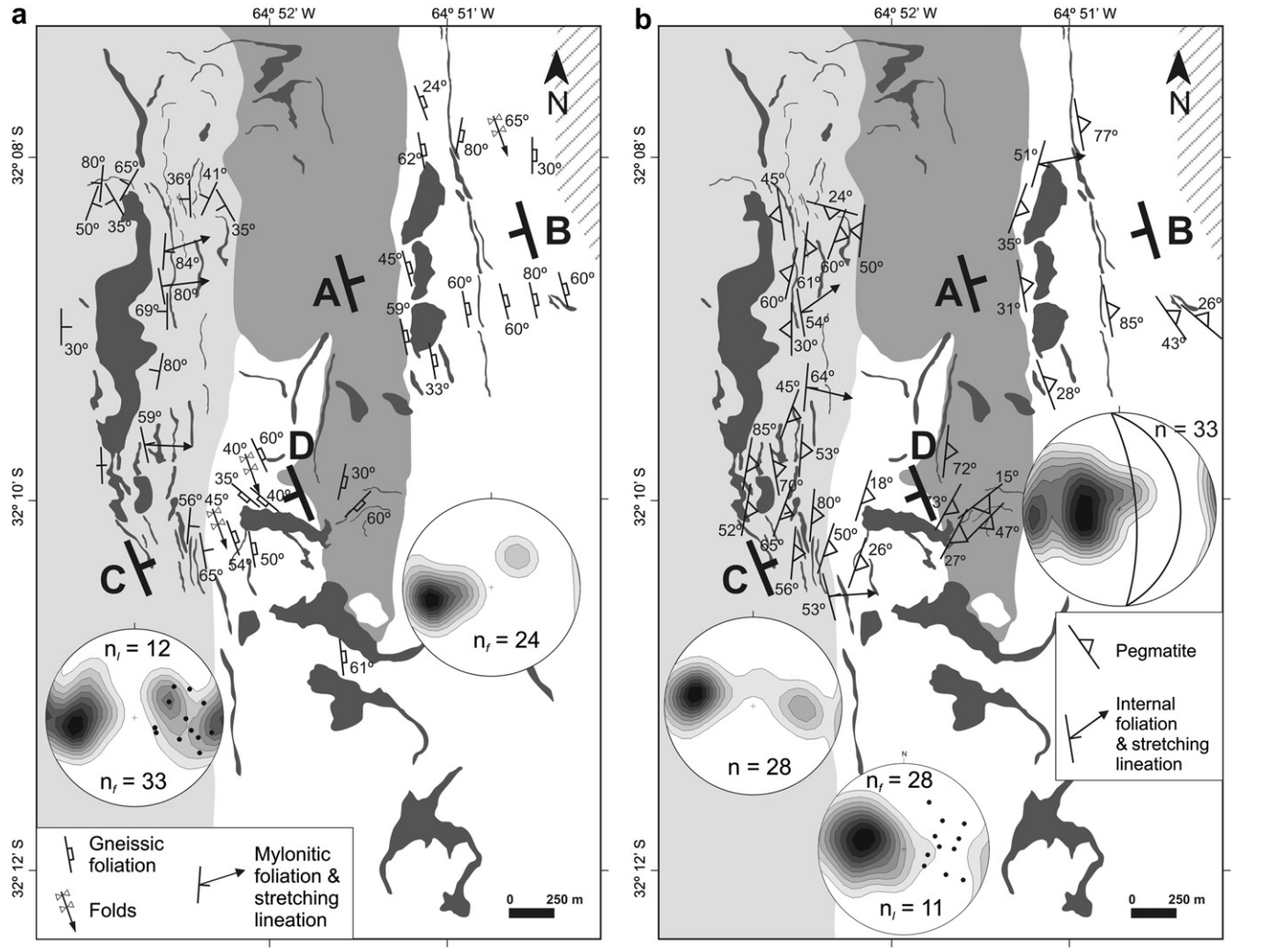

Fig. 8. Structural maps of the LSD. a) Mylonitic foliation measurements and lower-hemisphere stereograms showing poles to mylonitic foliation planes (density diagrams) and mineral-stretching lineation (dots), in both the eastern part of the LSD and in the TZ. b) Orientation of pegmatite-country rock contacts and lower-hemisphere stereograms showing data from both the eastern part of the LSD and the TZ. Poles to mylonitic foliation and mineral-stretching lineation (dots) of pegmatites are also shown together in the same lower-hemisphere stereogram at the bottom of the map. *n*: number of pegmatite orientation measurements; n_f: number of mylonitic foliation measurements; n_l: number of stretching lineation measurements. Orientations and location of the cross-sections (A–B and C–D) represented in Fig. 9 are also indicated. Lithological references as in Fig. 3.

compressive stress (σ_3), analogous to T extensional fractures. On the other hand, the high-dip pegmatites are regarded as magmas that ascended through synthetic P-fractures (Fig. 10) that acted as feeding channels, transferring magmas from below. The interconnection between different fracture systems constituted a very effective mechanism for magma transport in the LSD. The temperature (700–750 °C) and pressure (500 MPa) conditions that operated during the motion of the GCSZ indicate that this structure was formed at middle crustal levels, below the brittle–ductile transition. The GCSZ was therefore in a favorable setting to build up pressures able to generate the embrittlement of the country rocks and, consequently, an effective upward migration of pegmatitic melts through fractures. The high volatile content of these pegmatites would enhance a valve mechanism characterized by alternating periods of melt retention during ductile shearing of the country rocks and melt escape due to transient hydraulic fracturation events.

5.3. Magma pumping

The conspicuous angular correlation between the mylonitic foliation and the orientation of the pegmatite bodies measured all over the HSD, even where mylonitic foliation changes its orientation, evidences a close relationship between the mylonitic foliation pattern and the generation of space for the ascent and emplacement of the pegmatitic melts. The low viscosity and overpressurized conditions of the volatile-rich pegmatite melts can overcome the tensile stress of anisotropic country rocks, leading to the fast ascent of the melts through conduits parallel to either the mylonitic foliation or P-fractures (Fig. 10). A part of these ascending melts have been stagnated in such high-dip conduits, which explains the abundance of pegmatite sheets concordant with the mylonitic foliation or P-type fractures (Fig. 6). The low-dip pegmatites (Figs. 8b and 9) cannot be explained in the same way, as their orientation is rather compatible with emplacement along minor C′-shear zones or T-fractures (Fig. 10). During ongoing deformation, the mylonitic foliation and P-fractures can be reactivated as shear zones, while the low-dip surfaces of anisotropy (C′-planes or T-fractures) might behave as releasing bends connecting adjacent shear zones (Fig. 11). Displacements along staggered shear zones with releasing bends induce the local development of domains with negative pressure gradients, where open spaces could form transiently (Fig. 11a and b). We contend that these spaces acted as effective attractors for the collection of buoyant melts, a mechanism similar to “magma pumping” (Fig. 11c–e). At

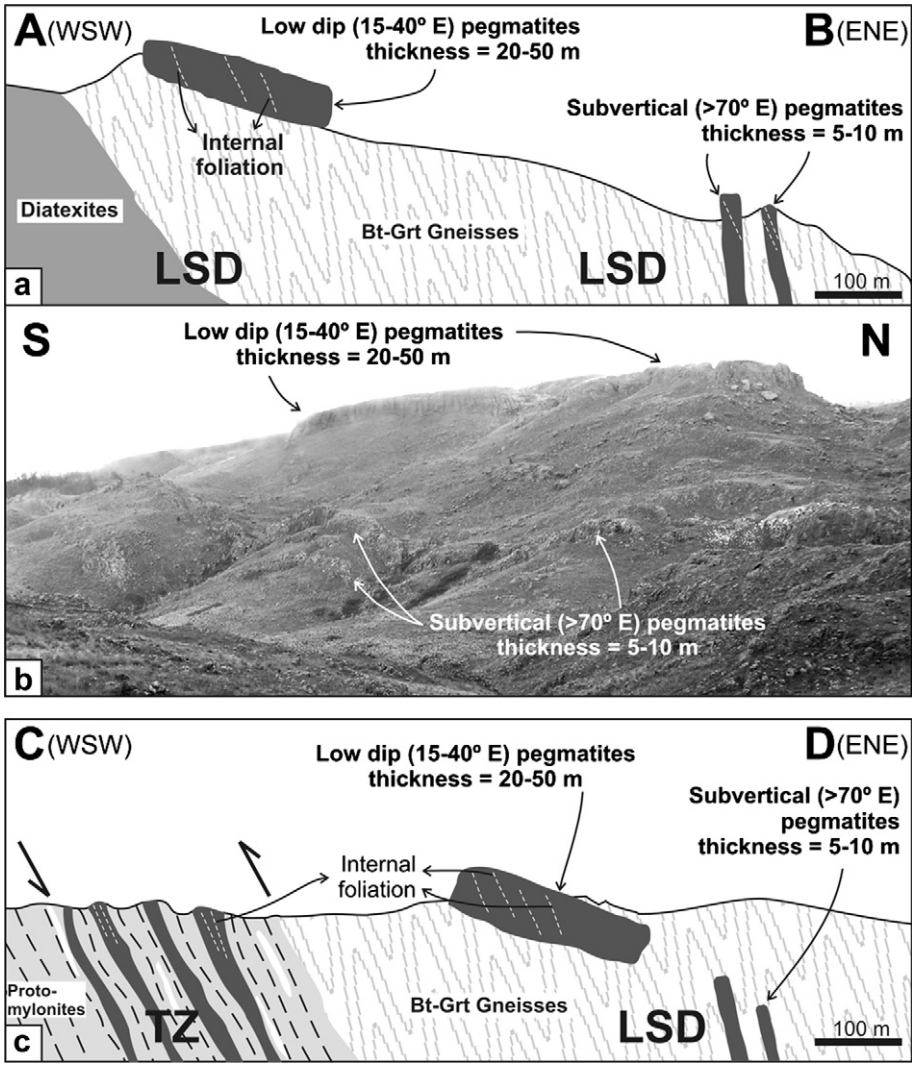

Fig. 9. Structural relationships between low- and high-dip pegmatites in the LSD. a) WSW–ENE cross-section AB (see Fig. 8 for localization) and field photograph of the same outcrops viewed in a N–S section, where field relationship can be observed; photograph width is 1500 m long. c) WSW–ENE cross-section CD (Fig. 8) concerning both the low strain domain and the transition zone.

a much larger scale, magma pumping could be equivalent to the volatile-driven intrusion mechanism for the pervasive, millimeter-scale migration of magmas in anatectic zones, as proposed by Weinberg et al. (2009). The accumulation of volatile-rich melts is an efficient way to open hydraulic fractures in ductile country rocks by melt-enhanced embrittlement processes (Davidson et al., 1994; Esteban et al., 2008). Melt-enhanced embrittlement and contact heating work together in the weakening of the country rocks around the less-pressurized upper tips of the places where magma is emplaced (Fig. 11e). In this way, the volatile-rich pegmatitic melts also favor steady reactivations of releasing bridges in which the magma is pumped.

As seen in many outcrops, multiple sheets of pegmatite are closely stacked on each other (Figs. 4 and 5). This field observation supports the sequential injection of independent batches of pegmatitic melt. Fig. 11 represents the formation of a composite pegmatite body by the stacking of several igneous sheets constructed by the mechanism of magma pumping. Emplacement sites are continuously opened at an oblique angle with respect to the main mylonitic foliation or shear zones (Fig. 11a and b), and pegmatitic lenses are progressively arranged in larger, composite tabular-shaped bodies parallel to the mylonitic foliation (Fig. 11c–e). As shown in Figs. 5 and 11, the mylonitic foliation of the country rocks is deflected around the pegmatitic bodies frequently, suggesting that the growth of such bodies was partly promoted by the high overpressure of the melts. In short, we document what we believe to be the first report of composite pegmatitic bodies emplaced in a contractional setting. Each independent sheet of the pegmatitic stack was mainly formed by a mechanism of permited intrusion (Fig. 11c) with a minor contribution of forcedly emplacement mechanism (Fig. 11e).

The magma pumping mechanism (Fig. 11) is analogous to that proposed by D'Lemos et al. (1992) for strike-slip shear zones. According to these authors, magmas moved up from underlying anatectic zones aided by their own buoyancy and entered into extensional jogs generated during development of an anastomosing strike-slip shear zone.

The GCSZ in southern CPF could be seen as representing an ancient magma transfer zone, similar to that defined by Moyen et al. (2003) in the Closepet batholith of southern India, where magmas were transported to higher structural levels feeding upper-crustal plutons above the current erosion level. However, unlike the granites of the Closepet batholith, volatile-rich pegmatitic melts such as those outcropping in the southern CPF would

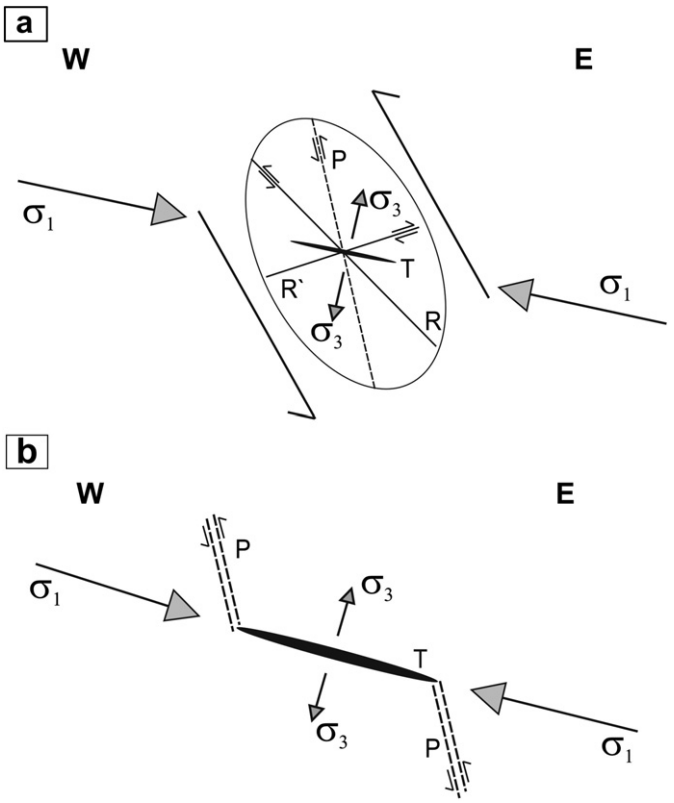

Fig. 10. Schematic model for space generation. a) Spaces develop in a shear zone according to the Riedel model of fracturation. b) Highly dipping pegmatites are consistent with P-shear fractures. These fractures were able to act as feeding channels for low-dipping and thicker pegmatites emplaced along extensional T-fractures.

have been cooled to their solidus within a few years or months (e.g., Webber et al., 1999; London, 2005, and references therein). Therefore, they are not expected to ascent much above the presently exposed structural level.

The intrusion of pegmatites took place during the overall deformation process. Within the HSD and the TZ, many of the initially emplaced pegmatites developed a mylonitic foliation (Fig. 5e) and experienced rotations during subsequent shearing. The intensity of rotations depends on the emplacement mechanism. The fracture-controlled pegmatites were emplaced along P-fractures (Fig. 10) and, consequently, only need slight rotations to become parallel to the shear plane (Fig. 12). In contrast, the pegmatites produced by magma pumping were emplaced along T-fractures (Fig. 10) and with further shearing some of them experienced large rotations leading to the development of tight folds (Figs. 5f and 12). Some W-dipping pegmatites with mylonitic foliation, like that represented by the Fig. 5e, could correspond to pegmatites emplaced in R′-fractures that were rotated slightly after its emplacement (Fig. 12). Late pegmatites emplaced by either of the two mechanisms in the HSD and the TZ have retained their original orientations (Fig. 12).

Pegmatites of the LSD are regarded as magmas intruded in fractures that experienced almost no rotation. We explain this lack of noticeable rotation and shearing by the relatively short time and low strain rate that took place in the LSD, hence preserving the initial stages of pegmatite intrusion. The HSD and LSD can be considered as complementary domains affected by different degrees of the same deformational event. Consequently, different magma transport mechanisms took place in both domains, depending on rotation and shear intensity.

No fracture system of the simple shear model consistent with the stress field of the GCSZ (Fig. 10) can explain the formation of either the discordant, steeply W-dipping and foliation-free pegmatites found in the HSD and the LSD, or the rare discordant pegmatites with E–W strike and steep dips observed in the LSD. These geometries are consistent with emplacements as

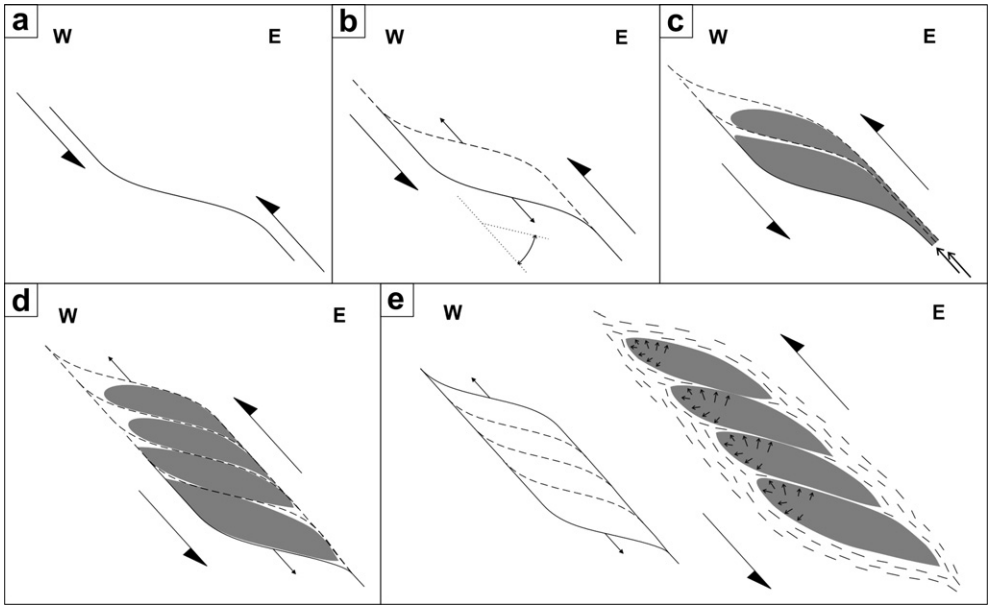

Fig. 11. Schematic model explaining space generation by magma-pumping in the HSD. a and b) Generation of potential spaces by opening of releasing bends during motion along curved shear zones. c) After crystallization of the pegmatitic melt that initially replenishes the space, the bend geometry is maintained. d) The repeated interplay between successive shearing events and melt supply can explain the development of stacks of pegmatite lenses, which display deformation at high-temperature conditions in their fringe zones. e) Final arrangement of a stack of pegmatitic lenses, harmonically deflecting the surrounding mylonitic foliation. The arrows mark the local deformation of the country rocks, induced for the concentration of over-pressurized fluids at the upper tip of each lens.

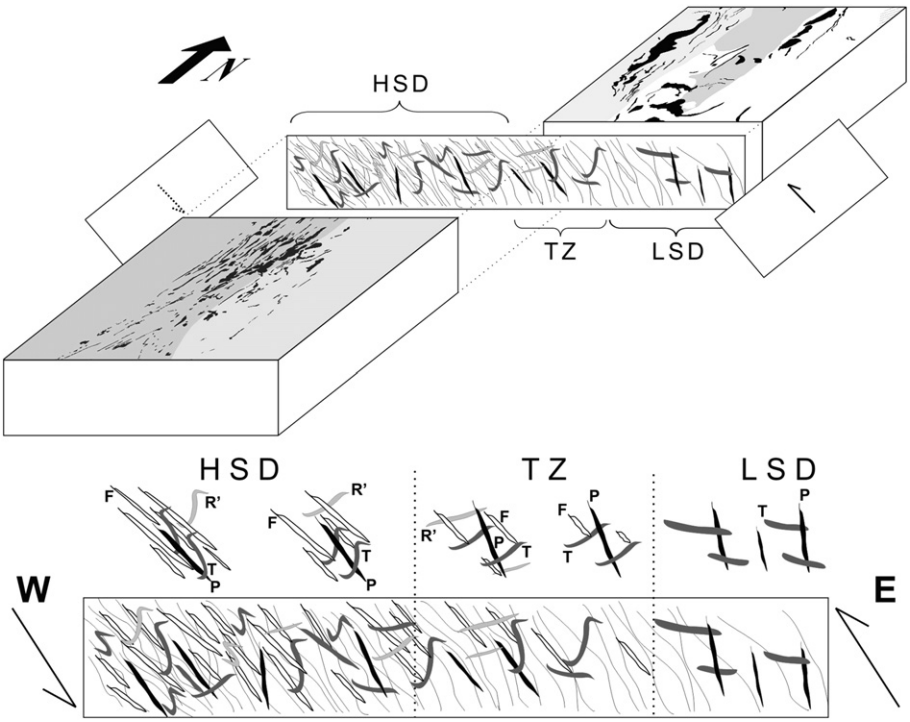

Fig. 12. 3D sketch of the southern CPF, where observations from the LSD, TZ, and HSD are integrated. Pegmatitic melts emplaced by both fracture-controlled and magma pumping mechanisms are schematically shown in the representative cross-section. Scheme is not to scale. The LSD preserves the original position of the pegmatitic intrusions while in the HSD the stronger deformation resulted in the reorientation of most of the pegmatitic sheets toward the main shear plane. F: mylonitic foliation; P, R′ and T: Paterson, Riedel and tension fractures, respectively.

Andersonian dykes (Anderson, 1951), provided the main stress axis be vertical. We propose that such pegmatites represent late magmatic pulses that were emplaced during short episodes of tectonic quiescence, when transient shifts of the main stress axis to the upright position took place. Such a scenario favors the development of the vertical tension cracks required for the emplacement of the discordant pegmatites. Accordingly, the high-dip discordant pegmatites could be the expression of such short-lived extensional events within the overall contractional history of the GCSZ. The presence of northward- and eastward-trending discordant pegmatites could reflect the extension that takes place parallel and perpendicular to the belt, once thickened by the reverse GCSZ, a common feature in orogenic belts undergoing extensional collapse subsequent to crustal thickening. Further studies will test if this last interpretation is correct, by looking for additional structural evidence on the extensional tectonics.

6. Conclusions

Shear zones constitute efficient anisotropies in the continental crust, able to provide spaces for magma transfer from lower to middle crustal levels. In the GCSZ, the huge amount of pegmatitic melts that concentrated toward the higher strain domains demonstrates the close relationship existing between magma transport and deformation. Two mechanisms for pegmatite ascent and emplacement have been recognized in the Comechingones pegmatitic field: magma pumping and fracture-controlled mechanisms. The contrasted pegmatite content of both strain domains (85% in the high strain domain versus 15% in the low strain domain) strongly suggests that magma pumping was particularly efficient in catching the pegmatite melts within the deeper HSD. We also propose that sliding along the mylonitic foliation also contributed to the ascent and emplacement of pegmatitic melts, thus nucleating and enhancing further deformation of the GCSZ. Finally, we propose that progressive deformation and emplacement of pegmatite takes place in a feedback relationship, a conclusion that could represent a tool for the exploration of pegmatite-related metallic and non-metallic deposits.

Acknowledgments

This work is part of the doctoral research of M. Demartis, who was supported by CONICET. It was supported by “Agencia Nacional de Promoción Científica y Técnica” (ANPCyT) and SeCyT-Universidad Nacional de Río Cuarto (project PICT-2008-1477), CONICET (project PIP-CONICET-0916), and SeCyT-Universidad Nacional de Río Cuarto (program 18/C 360). J. M. Tubía acknowledges support by CGL2010-14869 project (Ministerio de Ciencia e Innovación) and by the research group IT-364-10 (Gobierno Vasco). We sincerely thank Jean Luc Bouchez and Fernando Hongn for their constructive and careful reviews, which have helped to significantly improve the original manuscript. We wish to thank Fernando Cañas for his careful and helpful language assistance. Adriel Muñoz is also thanked for his invaluable contributions during both field and office operations.

References

Alfonso, P., Melgarejo, J.C., Yusta, I., Velasco, F., 2003. Geochemistry of feldspars and muscovite in granitic pegmatite from the Cap de Creus field, Catalonia, Spain. The Canadian Mineralogist 41, 103–116.

Anderson, E.M., 1951. The Dynamics of Faulting and Dyke Formation, with Applications to Britain, Second ed. Oliver and Boyd, Edinburgh, 206 pp.

Araújo, M.N.C., Alves da Silva, F.C., Jardim de Sá, E.F., 2001. Pegmatite emplacement in the Seridó belt, northeastern Brazil: late-stage kinematics of the Brasiliano orogen. Gondwana Research 4, 75–85.

Baker, D.R., 1998. Granite melt viscosity and dike formation. Journal of Structural Geology 20, 1395–1404.

Bouchez, J.L., Delas, C., Gleizes, G., Nédélec, A., Cuney, M., 1992. Submagmatic microfractures in granites. Geology 20, 35–38.
Brisbin, W.C., 1986. Mechanics of pegmatite intrusion. American Mineralogist 71, 644–651.
Brown, M., Solar, G.S., 1998a. Shear-zone systems and melts: feedback relations and self-organization in orogenic belts. Journal of Structural Geology 20, 211–227.
Brown, M., Solar, G.S., 1998b. Granite ascent and emplacement. Shear-zone systems and melts: feedback relations and self-organization in orogenic belts. Journal of Structural Geology 20, 211–227.
Brown, M., Solar, G.S., 1999. The mechanism of ascent and emplacement of granite magma during transpression: a syntectonic granite paradigm. Tectonophysics 312, 1–33.
Burda, J., Gawęda, A., 2009. Shear-influenced partial melting in the Western Tatra metamorphic complex: geochemistry and geochronology. Lithos 110, 373–385.
Chadwick, R.A., 1958. Mechanisms of pegmatite emplacement. Bulletin of the Geological Society of America 69, 803–836.
Corti, G., Bonini, M., Mazzarini, F., Boccaletti, M., Innocenti, F., Manetti, P., Mulugeta, G., Sokoutis, D., 2002. Magma-induced strain localization in centrifuge models of transfer zones. Tectonophysics 348, 205–218.
Černý, P., 1991a. Rare-element granitic pegmatites. Part I: anatomy and internal evolution of pegmatite deposits. Geoscience Canada 18, 49–67.
Černý, P., 1991b. Rare-element granitic pegmatites. Part II: regional to global environments and petrogenesis. Geoscience Canada 18, 68–81.
Černý, P., Ercit, T.S., 2005. The classification of granitic pegmatites revisited. The Canadian Mineralogist 43, 2005–2026.
Černý, P., Meintzer, R.E., Anderson, A.J., 1985. Extreme fractionation in rare-element granitic pegmatites: selected examples of data and mechanisms. The Canadian Mineralogist 23, 381–421.
Černý, P., Brisbin, W.C., 1982. The Osis Lake pegmatitic granite, Winnipeg River District, southeastern Manitoba. In: Černý, P. (Ed.), Granitic Pegmatites in Science and Industry. Short Course Handbook, vol. 8. Mineralogical Association of Canada, pp. 545–555.
D'Lemos, R.S., Brown, M., Strachan, R.A., 1992. Granite magma generation, ascent and emplacement within a transpressional orogen. Journal of the Geological Society, London 149, 487–490.
Davidson, C., Schmid, S.M., Hollister, L.S., 1994. Role of melt during deformation in the deep crust. Terra Nova 6, 133–142.
Demartis, M., 2010. Emplazamiento y petrogénesis de las pegmatitas y granitoides asociados. Sector central de la Sierra de Comechingones, Córdoba, Argentina. PhD Thesis, Universidad Nacional de Río Cuarto, Argentina.
Demartis, M., Melgarejo Draper, J.C., Alfonso, P., Coniglio, J.E., Pinotti, L.P., D'Eramo, F.J., 2011. Mineralogy of a Highly Fractionated Replacement Unit from "Ángel" Pegmatite, Comechingones Pegmatitic Field, Córdoba, 14. Asociación Geológica Argentina, Argentina. Serie D, Special Publication N°69–70.
Denèle, Y., Olivier, P., Gleizes, G., 2008. Progressive deformation of a zone of magma transfer in a transpressional regime: the Variscan Mérens shear zone (Pyrenees, France). Journal of Structural Geology 30, 1138–1149.
Dingwell, D.B., Hess, K.U., Knoche, R., 1996. Granite and granitic pegmatite melts: volumes and viscosities. Transactions of the Royal Society of Edinburgh: Earth Sciences 87, 65–72.
Druguet, E., Hutton, D.H.W., 1998. Syntectonic anatexis and magmatism in a mid-crustal transpressional shear zone: an example from the Hercynian rocks of the eastern Pyrenees. Journal of Structural Geology 20, 905–916.
Esteban, J.J., Cuevas, J., Vegas, N., Tubía, J.M., 2008. Deformation and kinematics in a melt-bearing shear zone from the Western Betic Cordilleras (Southern Spain). Journal of Structural Geology 30, 380–393.
Fagiano, M., 2007. Geología y Petrología del basamento cristalino de las Albahacas, sur de la Sierra de Comechingones, Córdoba. PhD Thesis, Universidad Nacional de Río Cuarto, Argentina.
Galliski, M., 1994. La Provincia Pegmatítica Pampeana. I: Tipología y distribución de sus distritos económicos. Revista de la Asociación Geológica Argentina 49, 99–112.
Galliski, M.A., Černý, P., 2006. Geochemistry and structural state of columbite-group minerals in granitic pegmatites of the Pampean ranges, Argentina. The Canadian Mineralogist 44, 645–666.
Henderson, I.H.C., Ihlen, P.M., 2004. Emplacement of polygeneration pegmatites in relation to Sveco-Norwegian contractional tectonics: examples from southern Norway. Precambrian Research 133, 207–222.
Hutton, D.H.W., 1988. Granite emplacement mechanisms and tectonic controls: inferences from deformation studies. Transactions of the Royal Society of Edinburgh: Earth Sciences 79, 245–255.
Kontak, D.J., 2006. Nature and origin of an LCT-suite pegmatite with late-stage sodium enrichment, Brazil Lake, Yarmouth County, Nova Scotia. I. Geological setting and petrology. The Canadian Mineralogist 44, 563–598.
Leitch, A.M., Weinberg, R.F., 2002. Modelling granite migration by mesoscale pervasive flow. Earth and Planetary Science Letters 200, 131–146.
London, D., 1986a. The magmatic-hydrothermal transition in the Tanco rare-element pegmatite: evidence from fluid inclusions and phase equilibrium experiments. American Mineralogist 71, 376–395.
London, D., 1986b. Formation of tourmaline-rich gem pockets in miarolitic pegmatites. American Mineralogist 71, 396–405.
London, D., 1992. The application of experimental petrology to the genesis and crystallization of granitic pegmatites. The Canadian Mineralogist 30, 499–540.
London, D., 2005. Granitic pegmatites: an assessment of current concepts and directions for the future. Lithos 80, 281–303.
Martino, R., 2003. Las fajas de deformación dúctil de las Sierras Pampeanas de Córdoba: Una reseña general. Revista de la Asociación Geológica Argentina 58, 549–571.
Moyen, J.F., Nédélec, A., Martin, H., Jayananda, M., 2003. Syntectonic granite emplacement at different structural levels: the Closepet granite, South India. Journal of Structural Geology 25, 611–631.
Nabelek, P.I., Whittington, A.G., Sirbescu, M.C., 2010. The role of H_2O in rapid emplacement and crystallization of granite pegmatites: resolving the paradox of large crystals in highly undercooled melts. Contributions to Mineralogy and Petrology 160, 313–325.
Neves, S.P., Vauchez, A., 1995. Magma emplacement and shear zone nucleation and development in northeast Brazil (Fazenda Nova and Pernambuco shear zones; State of Pernambuco). Journal of South American Earth Sciences 8, 289–298.
Neves, S.P., Vauchez, A., Archanjo, C.J., 1996. Shear zone-controlled magma emplacement or magma-assisted nucleation of shear zones? Insights from northeast Brazil. Tectonophysics 262, 349–364.
Ninomiya, Y., 2004. Lithologic mapping with multispectral ASTER TIR and SWIR data. Sensors, Systems, and Next-Generation Satellites VII 5234, 180–190.
Otamendi, J.E., Castelarini, P.A., Fagiano, M., Demichelis, A., Tibaldi, A., 2004. Cambrian to Devonian geologic evolution of the Sierra de Comechingones, eastern Sierras Pampeanas: evidence for the development and exhumation of continental crust on the proto-pacific margin of Gondwana. Gondwana Research 7, 1143–1155.
Partington, G.A., 1990. Environment and structural controls on the intrusion of the giant rare metal greenbushes pegmatite, Western Australia. Economic Geology 85, 437–456.
Passarelli, C.R., Basei, M.A.S., Siga Jr., O., Reath, I.M., Campos Neto, M.D.C., 2010. Deformation and geochronology of syntectonic granitoids emplaced in the major Gercino shear zone, southeastern South America. Gondwana Research 17, 688–703.
Pinotti, L.P., Tubía, J.M., D'Eramo, F.J., Vegas, N., Sato, A.M., Coniglio, J.E., Aranguren, A., 2006. Structural interplay between plutons during the construction of a batholith (Cerro Aspero batholith, Sierras de Córdoba, Argentina). Journal of Structural Geology 28, 834–849.
Rapela, C.W., Pankhurst, R.J., Casquet, C., Baldo, E., Saavedra, J., Galindo, C., Fanning, C.M., 1998. The Pampean orogeny of the southern proto-Andes: Cambrian continental collision in the Sierras de Córdoba. In: Pankhurst, R.J., Rapela, C.W. (Eds.), The Proto-Andean Margin of Gondwana. Geological Society, London, pp. 181–217. Special Publication 142.
Rapela, C.W., Casquet, C., Baldo, E., Dahlquist, J., Pankhurst, R.J., Galindo, C., Saavedra, J., 2001. Las Orogénesis del Paleozoico Inferior en el margen proto-andino de América del Sur, Sierras Pampeanas, Argentina. Journal of Iberian Geology 27, 23–41.
Roda, E., Pesquera, A., Fontan, F., Keller, P., 2004. Phosphate mineral associations in the Cañada pegmatite (Salamanca, Spain): paragenetic relationships, chemical compositions, and implications for pegmatite evolution. American Mineralogist 89, 110–125.
Rosenberg, C.L., 2004. Shear zones and magma ascent: a model based on a review of the tertiary magmatism in the Alps. Tectonics 23. doi:10.1029/2003TC001526 TC3002.
Rowan, L.C., Mars, J.C., 2003. Lithologic mapping in the mountain pass, California area using advanced spaceborne thermal emission and reflection radiometer (ASTER) data. Remote Sensing of the Environment 84, 350–366.
Simpson, C., Law, R.D., Gromet, L.P., Miró, R., Northrup, C.J., 2003. Paleozoic deformation in the Sierras de Córdoba and Sierras de Las Minas, eastern Sierras Pampeanas, Argentina. Journal of South American Earth Science 15 (7), 749–764.
Stern, L.A., Brown Jr., G.E., Bird, D.K., Jahns, R.H., Foord, E.E., Shigley, J.E., Spaulding Jr., L.B., 1986. Mineralogical and geochemical evolution of the little three pegmatite-aplite layered intrusive, Ramona, California. American Mineralogist 71, 406–427.
Stilling, A., Černý, P., Vanstone, P.J., 2006. The Tanco pegmatite at Bernic Lake, Manitoba. XVI. Zonal and bulk compositions and their petrogenetic significance. The Canadian Mineralogist 44, 599–623.
Stipp, M., Stünitz, H., Heilbronner, R., Schmid, S.M., 2002. The eastern Tonale fault zone: a 'natural laboratory' for crystal plastic deformation of quartz over a temperature range from 250 to 700 °C. Journal of Structural Geology 24, 1861–1884.
Vigneresse, J.L., 1995. Control of granite emplacement by regional deformation. Tectonophysics 249, 173–186.
Webber, K.L., Simmons, W.B., Falster, A.U., Foord, E.E., 1999. Cooling rates and crystallization dynamics of shallow level pegmatite-aplite dikes, San Diego County, California. American Mineralogist 84, 708–717.
Weinberg, R.F., Regenauer-Lieb, K., 2010. Ductile fractures and magma migration from source. Geology 38, 363–366.
Weinberg, R.F., Sial, A.N., Mariano, G., 2004. Close spatial relationship between plutons and shear zones. Geology 32, 377–380.
Weinberg, R.F., Mark, G., Reichardt, H., 2009. Magma ponding in the Karakoram shear zone, Ladakh, NW India. Geological Society of America Bulletin 121, 278–285.
Whitmeyer, S.J., Simpson, C., 2003. High strain-rate deformation fabrics characterize a kilometers-thick Paleozoic fault zone in the Eastern Sierras Pampeanas, central Argentina. Journal of Structural Geology 25, 909–922.